magnetochemistry

MDPI

Article

Comparison of Current Induced Domain Wall Motion Driven by Spin Transfer Torque and by Spin Orbit Torque in Ferrimagnetic GdFeCo Wires

Pham Van Thach [1,*], Satoshi Sumi [2], Kenji Tanabe [2] and Hiroyuki Awano [2,*]

[1] Institute of Materials Science, Vietnam Academy of Science and Technology, 18 Hoang Quoc Viet, Hanoi 100000, Vietnam
[2] Toyota Technological Institute, Tempaku, Nagoya 468-8511, Japan; sumi@toyota-ti.ac.jp (S.S.); tanabe@toyota-ti.ac.jp (K.T.)
* Correspondence: thachpv@ims.vast.ac.vn (P.V.T.); awano@toyota-ti.ac.jp (H.A.)

Abstract: Current-induced domain wall motion (CIDWM) in magnetic wires can be driven by spin transfer torque (STT) originating from transferring angular momentums of spin-polarized conducting electrons to the magnetic DW and can be driven by spin orbit torque (SOT) originating from the spin Hall effect (SHE) in a heavy metal layer and Dzyaloshinsky Moriya (DMI) generated at an interface between a heavy metal layer and a magnetic layer. In this work, we carried out a comparative study of CIDWM driven by STT and by SOT in ferrimagnetic GdFeCo wires with magnetic perpendicular anisotropy based on structures of SiN (10 nm)/GdFeCo (8 nm)/SiN (10 nm) and Pt (5 nm)/GdFeCo (8 nm)/SiN (10 nm). We found that CIDWM driven by SOT exhibited a much lower critical current density (J_C), and much higher DW mobility (μ_{DW}). Our work might be useful for the realization and the development of low-power and high-speed memory devices.

Keywords: current-induced domain wall motion; ferrimagnets; spin transfer torque; spin orbit torque

Citation: Thach, P.V.; Sumi, S.; Tanabe, K.; Awano, H. Comparison of Current Induced Domain Wall Motion Driven by Spin Transfer Torque and by Spin Orbit Torque in Ferrimagnetic GdFeCo Wires. *Magnetochemistry* **2024**, *10*, 36. https://doi.org/10.3390/magnetochemistry10050036

Academic Editors: Paula Corte-Leon and Ahmed Talaat

Received: 12 March 2024
Revised: 5 May 2024
Accepted: 13 May 2024
Published: 19 May 2024

1. Introduction

Current-induced domain wall motion (CIDWM) in magnetic wires has attracted much attention in the spintronic field over the past decade due to its potential applications such as magnetic memory and logic devices [1–5]. In particular, novel magnetic memory is so-called race-track memory, where digital data are stored in DWs in the magnetic wires [6]. To realize a magnetic memory with low power consumption and high operation speed, a fast CIDWM at a low current density is required. Initial studies were mainly focused on magnetic wires with in-plane anisotropy, typically NiFe wires [7–9]. Then, interest was devoted to magnetic wires with perpendicular anisotropy such as Co/Ni and Co/Pt wires [10–14] because magnetic wires with perpendicular anisotropy possess narrower DWs, which is preferable for high-density magnetic storage. CIDWM can be driven by spin transfer torque (STT) originating from transferring angular momentums of spin-polarized conducting electrons to DWs and can be driven by spin orbit torque (SOT) originating from the spin Hall effect (SHE) in a heavy metal layer and Dzyaloshinsky Moriya interaction (DMI) generated at an interface between a heavy metal layer and a magnetic layer. In addition, STT only can drive the DWs against the current–flow direction, while SOT can drive the DWs against and along the current–flow direction [15–19].

Lately, CIDWM in rare-earth transition metal (RE-TM)-based ferrimagnetic wires with magnetic perpendicular anisotropy (PMA) has been extensively investigated because fast DW dynamic at the angular momentum compensation point has been observed in these ferrimagnetic wires [20–24]. In fact, the ferrimagnetic material has exhibited higher DW mobilities compared to other magnetic materials [20–23]. Although field assisted CIDWM driven by STT and CIDWM driven by SOT in ferrimagnetic GdFeCo wires have been well

studied in earlier works [23,25,26], there is still no report on a comparison of CIDWM driven by STT and driven by SOT in such ferrimagnetic GdFeCo wires.

For this work, we have performed a comparative study of CIDWM driven by STT and driven by SOT in ferrimagnetic GdFeCo wires based on structures of SiN (10 nm)/GdFeCo (8 nm)/SiN (10 nm) and Pt (5 nm)/GdFeCo (8 nm)/SiN (10 nm). Our results have identified that DW motion driven by SOT exhibited much lower critical current density and higher DW mobility. Moreover, this study has highlighted the essential role of the heavy metal layer for realizing CIDWM with a low critical current density and high DW mobility in ferrimagnetic GdFeCo wires.

2. Materials and Methods

Multilayers with structures of SiN (10 nm)/GdFeCo (8 nm)/SiN (10 nm) and Pt (5 nm)/GdFeCo (8 nm)/SiN (10 nm) were deposited on thermally oxidized silicon substrates by dc and rf magnetron sputtering at a base pressure of ~3×10^{-8} Torr. The sample structure is illustrated in Figure 1. Here, SiN is used as a seed layer and a capping layer. The Pt heavy metal layer works as a spin current source induced by the spin Hall effect (SHE), which can provide a spin torque that drives the chiral Néel walls stabilized by the DMI at the Pt/GdFeCo interface. The GdFeCo layers were fabricated by co-sputtering from Gd and $Fe_{75}Co_{25}$ targets. The composition of the GdFeCo alloy layer estimated from calibrated sputtering rates is $Gd_{26}Fe_{55.5}Co_{18.5}$. Patterned wires, 3 μm wide and 75 μm long, were fabricated using electron-beam lithography and the lift-off technique. The magnetic properties of the samples were characterized by anomalous Hall resistance measurement for the GdFeCo wires and vibrating sample magnetometer (VSM) for the GdFeCo films. The motion of DW in the GdFeCo wires was driven by single voltage pulses and directly observed using polar Kerr microscopy. All measurements were carried out at room temperature.

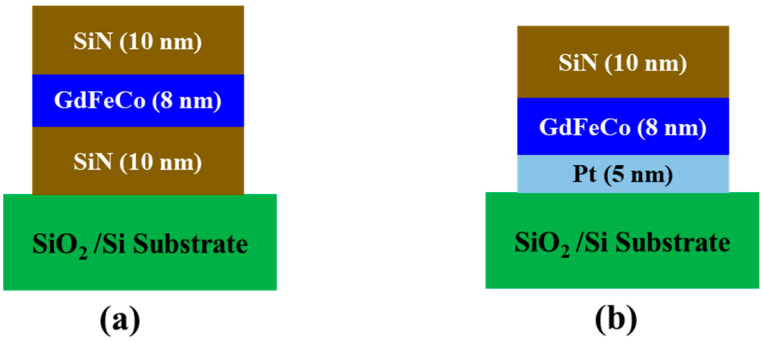

Figure 1. Schematic illustration of multilayered films with structures of (**a**) SiN (10 nm)/GdFeCo (8 nm)/SiN (10 nm); (**b**) Pt (5 nm)/GdFeCo (8 nm)/SiN (10 nm) deposited on a thermally oxidized silicon substrate.

3. Results and Discussion

Figure 2a shows a schematic illustration for measuring anomalous Hall resistances in the GdFeCo wires. A dc current of 1 mA was applied to the Hall bar. Hall voltages were detected from the other Hall bar under various external perpendicular magnetic fields. Anomalous Hall resistances were obtained from the detected Hall voltages divided by the applied current. The normalized hysteresis loops of the anomalous Hall resistances for the SiN/GdFeCo and Pt/GdFeCo wires are shown in Figure 2b. Rectangular hysteresis loops were obtained for the GdFeCo wires, clearly indicating a PMA of the wires. The coercive fields (H_C) were found to be ~19 mT for the SiN/GdFeCo wire and ~28 mT for the Pt/GdFeCo wire. The saturation magnetizations (M_S) of the SiN/GdFeCo and Pt/GdFeCo films measured by the VSM are ~3.3×10^4 A/m and ~3.8×10^4 A/m, respectively.

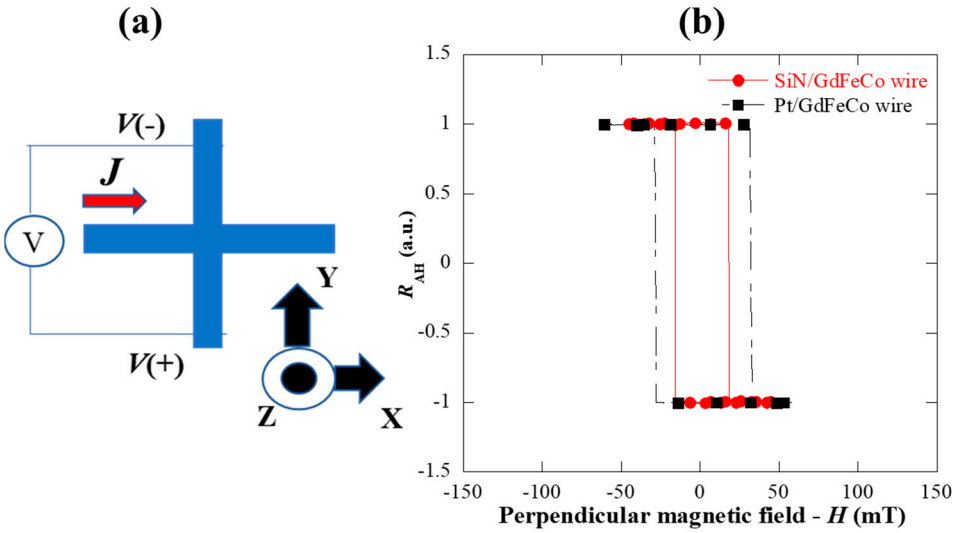

Figure 2. (**a**) Schematic illustration of anomalous Hall resistance measurement for the GdFeCo wires. Red arrow indicates the direction of current (J) flowing in the wires; (**b**) normalized anomalous Hall resistance (R_{AH}) of the SiN/GdFeCo and Pt/GdFeCo wires as a function of the perpendicular magnetic field (H).

We performed measurement of CIDWM in the SiN/GdFeCo and Pt/GdFeCo wires similarly to our earlier works [18,19,23]. An external out-of-plane magnetic field with amplitude much larger than the H_C of the GdFeCo wire was applied to saturate the wire magnetization. Then the magnetic field was gradually decreased and reversed its direction. By adjusting the amplitude of magnetic field precisely, a DW was nucleated in the wire. After nucleating and positioning the DW in the wire, the magnetic field was turned off. Next, the DW was displaced by applying a single voltage pulse to the wire, and the DW displacement was observed by polar Kerr microscopy. Current densities applied to the wire were calculated from the applied voltages, a measured value of wire resistance and the wire size. The measurement was repeated 5 times for each current density. The DW displacements in the wire were estimated using Kerr images in a differential mode. The DW velocity was calculated as ratio of the DW displacement/pulse width of applied voltage. Figure 3a,b present Kerr images before and after injecting a 100 ns-wide pulse current density of 4.3×10^{11}A/m^2 and 2.4×10^{11}A/m^2 into the SiN/GdFeCo and Pt/GdFeCo wires, respectively, as well as in a differential mode. Such images are typical examples for the observation of CIDWM in our samples. The Kerr images obviously show that the DW moved against the current direction for the SiN/GdFeCo wire and along the current direction for the Pt/GdFeCo wire, which indicates that STT drives DW motion for the SiN/GdFeCo wire and SOT drives DW motion for the Pt/GdFeCo wire [15–19].

STT is caused by a spin current inside the magnetic layer. In STT mechanism, when a spin-polarized electron current flows through the DW, the spin polarization direction of conducting electrons is aligned towards the magnetization of the DW due to the exchange interaction. Since the total spin momentum is conserved, spin angular momentum must be transferred to the magnetization of the DW, resulting in a torque called STT acting on the DW and displacing the DW along the electron flow (against the current flow) [27–29]. Unlike STT, SOT is rooted from a spin current induced by the spin Hall effect in the heavy metal layer. When an electrical current flows through the heavy metal/magnetic bilayer wire with the Néel DW, the spin current from the heavy metal layer diffuses into the magnetic layer, acting as a form of torque called SOT on the Néel DW. The direction of the DW motion depends on the sign of the spin Hall angle of the heavy metal layer as well as the chirality of the Néel DW. For the Pt/GdFeCo wire, the Pt has a positive spin Hall angle. Therefore, the DW is moved along the current flow when it is a left-handed chiral Néel DW [15,30,31].

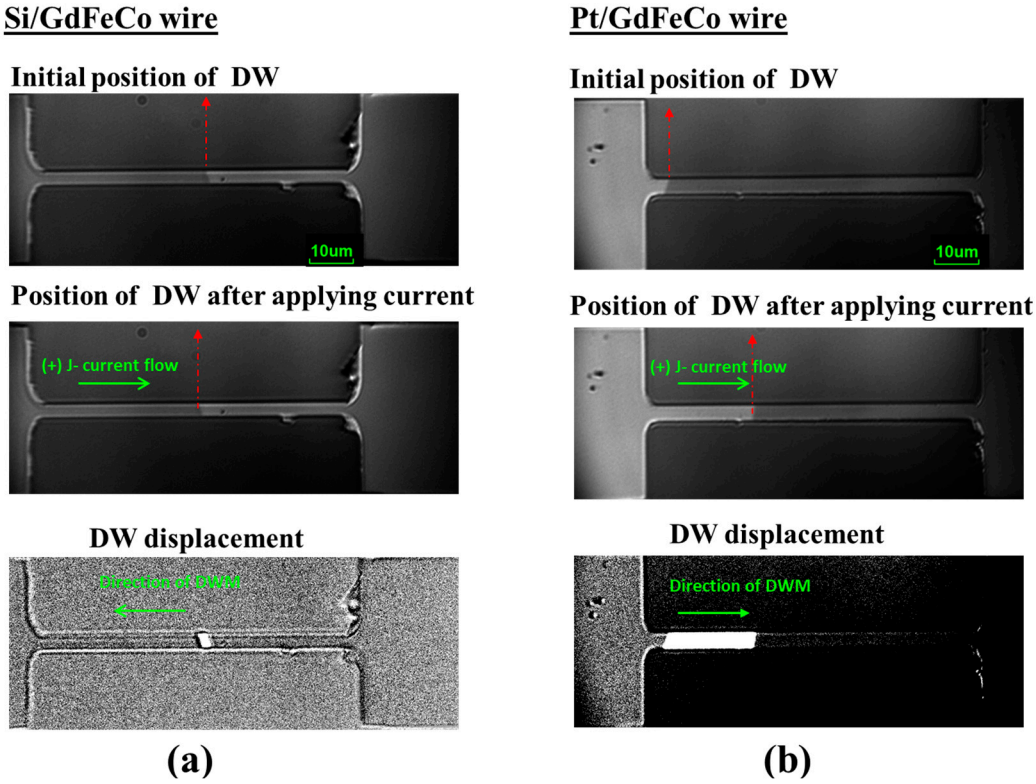

Figure 3. Polar Kerr images for observation of CIDWM in (**a**) the SiN/GdFeCo wire, (**b**) the Pt/GdFeCo wire. Upper images indicate the initial position of the DW as marked by the vertical dotted line. Middle images indicate the position of the DW as marked by the vertical dotted line after injecting a 100 ns-wide pulse current density of 4.3×10^{11} A/m^2 and 2.4×10^{11} A/m^2 to the SiN/GdFeCo and Pt/GdFeCo wires, respectively. Lower images are Kerr images in a differential mode, indicating the DW displacement.

In our experiment, we measured CIDWM in SiN/GdFeCo and Pt/GdFeCo wires by applying single-voltage pulses with a duration of 100 ns to the wires. Thus, the DW velocity was calculated as a DW displacement/100 ns. The DW velocity as a function of current density (J) for the SiN/GdFeCo and Pt/GdFeCo wires is summarized in Figure 4. As shown in Figure 4, the DW motion direction is opposite to the current direction for the SiN/GdFeCo wire and is the same as the current direction for the Pt/GdFeCo wire with all measured current densities. Note that the DW velocity is defined as positive when the DW direction is the same as the current direction. The maximum J that can be applied to the SiN/GdFeCo and Pt/GdFeCo wires for the observation of DW motion is almost similar (~4×10^{11} A/m^2). Nucleation of new domains starts to occur for current densities that are higher than the maximum current density, which may be due to current-induced weakening of the perpendicular anisotropy [21,32]. Remarkably, the critical current density (J_C), defined as the lowest applied current to induce DW motion in the Pt/GFeCo wire (J_C~1×10^{11} A/m^2), is about 3 times smaller than that of the SiN/GdFeCo wire (J_C~3×10^{11} A/m^2). In addition, the maximum DW velocity obtained for the Pt/GdFeCo wire is much higher than that for the SiN/GdFeCo wire at almost the same applied current density (J~4×10^{11} A/m^2). Next, DW mobility (μ_{DW} = DW velocity/current density) was estimated by fitting a linear line of the DW velocity vs. the current density. Here, the fitted data are in a measured current density range from ~3×10^{11} A/m^2 to ~4.3×10^{11} A/m^2 because DW motion is observed for both wires in this current density range. Estimated values of μ_{DW} are ~22×10^{-10} m^3/S·A for the Pt/GdFeCo wire, and ~-2.5×10^{-10} m^3/s·A for the SiN/GdFeCo wire. These results demonstrate that CIDWM driven by SOT has much greater efficiency than that driven by STT in the GdFeCo wire.

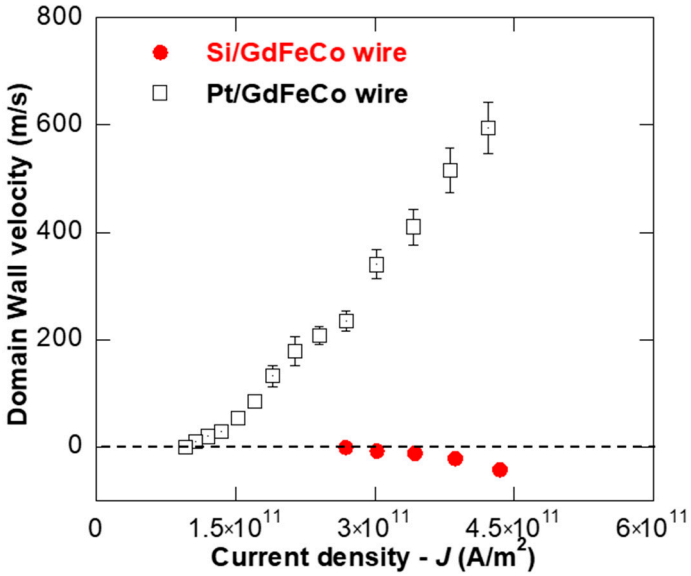

Figure 4. Dependence of DW velocity on current density for the SiN/GdFeCo and Pt/GdFeCo wires. Error bar represents the standard deviation of 5 independent measurements of DW velocity. Dash line indicates zero DW velocity ($v_{DW} = 0$).

It should be noted that the J_C for CIDWM driven by STT in Pt (2 nm)/TbFeCo (8 nm)/Pt (2 nm) wire is smaller for that driven by SOT in SiO_2/TbFeCo (8 nm)/Pt (2 nm) wire as observed in ref. [18], namely, J_C = ~1 × 10^{11} A/m^2 and ~1.3 × 10^{11} A/m^2 for CIDWM driven by STT and the one driven by SOT in the TbFeCo wire, respectively. However, the observed speed of the DW motion becomes faster for CIDWM driven by SOT in the high-current density range for this TbFeCo wire. It suggests that the DW motion driven by SOT in the TbFeCo/Pt wire is more effective in the high-current density range. On the other hand, the DW motion driven by STT in the Pt/TbFeCo/Pt wire is more effective in the low current density range where the DW begins to move, which may be due to the influence of heat from the upper and lower Pt layers.

To evaluate effective DMI field (H_{DMI}) and DMI constant (D) for the Pt/GdFeCo wire, we measured CIDWM in the GdFeCo wire under various longitudinal in-plane magnetic fields (H_X). It is reported that when the Néel DW stabilized by the DMI is displaced by the current under H_X, the DW velocity has a linear relationship with the magnitude of $|\boldsymbol{H}_X + \boldsymbol{H}_{DMI}|$ [15–17,33]. The DW velocity increases when H_X has the same sign as H_{DMI}. When H_X and H_{DMI} have opposite directions, then $|\boldsymbol{H}_X + \boldsymbol{H}_{DMI}|$ decreases, and the DW velocity decreases. If $\boldsymbol{H}_X = -\boldsymbol{H}_{DMI}$, the DW does not move. Furthermore, the direction of the DW motion can be changed if H_X is larger than H_{DMI} and their directions are opposite. Such a linear relationship is also observed in the Pt/GdFeCo wire. Thus, H_{DMI} was estimated by plotting the linear lines as shown in Figure 5. The estimated magnitude of H_{DMI} is ~236 mT. From the estimated H_{DMI}, D is calculated from the following expression: $D = \mu_O M_S H_{DMI} \Delta$, where μ_O is vacuum permeability, M_S is saturation magnetization, and Δ is DW width. Here, D of the Pt/GdFeCo wire was calculated using Δ = 12 nm from ref. [22]. The calculated value of D is ~0.11 mJ/m^2, which is consistent with the D values obtained in Pt/ferrimagnetic wires from refs. [22,33].

Lastly, essential parameters are summarized in Table 1 for a clear comparison of CIDWM driven by STT and by SOT in the GdFeCo wires. Those parameters, from some previous reports on other RE-TM-based ferrimagnetic wires, are also included in Table 1 for comparing this work with the previous works.

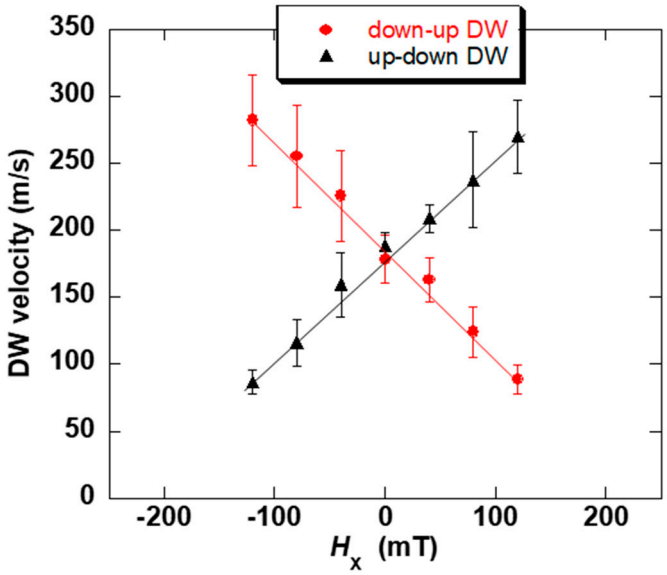

Figure 5. DW velocity as a function of the longitudinal in-plane magnetic field (H_X) of the Pt/GdFeCo wire under a current density of 2.1 × 10^{11} A/m^2. Circle and triangle symbols represent ↓↑ and ↑↓ DWs, respectively. Error bar represents the standard deviation of 5 independent measurements of DW velocity.

Table 1. Summary of estimated values of critical current density-J_C and DW mobility-μ_{DW} for this work and some previous works on other RE-TMs-based ferrimagnetic wires.

Sample Structure	J_C (×10^{11} A/m^2)	μ_{DW} (×10^{-10} m^3/S·A)	Mechanism	Reference
SiN/GdFeCo/SiN	~3	~−2.5	STT	This work
Pt/GdFeCo/SiN	~1	~22	SOT	This work
SiO_2/TbFeCo/Pt	~1.3	-	SOT	18
Pt/TbFeCo/Pt	~1	-	STT	18
Pt/TbCo/SiN	2.2–2.7	~5	SOT	21
Pt/GdCo/TaOx	3–6	~6.5	SOT	22

4. Conclusions

We have studied a comparison of CIDWM driven by STT in SiN (10 nm)/GdFeCo (8 nm)/SiN (10 nm) wire and driven by SOT in the Pt (5 nm)/GdFeCo (8 nm)/SiN (10 nm) wire. It was found that CIDWM driven by SOT in the Pt/GdFeCo wire revealed nearly 3 times smaller in the value of J_C and 9 times larger in the value of μ_{DW} than CIDWM driven by STT in the SiN/GdFeCo wire. Our work might be useful for the realization and the development of low-power and high-speed memory devices based on CIDWM in ferrimagnetic wires.

Author Contributions: Conceptualization, P.V.T. and H.A.; methodology, P.V.T., S.S., K.T. and H.A.; investigation, P.V.T. and S.S.; writing—original draft preparation, P.V.T. and H.A.; writing—review and editing, P.V.T., S.S., K.T. and H.A.; supervision, P.V.T. and H.A. All authors have read and agreed to the published version of the manuscript.

Funding: This research is funded by the Vietnam Academy of Science and Technology, under grant number KHCBVL.02/22-23.

Institutional Review Board Statement: Not applicable.

Informed Consent Statement: Not applicable.

Data Availability Statement: The data presented in this paper are available on request from the corresponding author.

Acknowledgments: This research was supported by Toyota Institute of Technology's Research Center for Smart Photons and Materials.

Conflicts of Interest: The authors declare no conflicts of interest.

References

1. Jaworowicz, J.; Vernier, N.; Ferré, J.; Maziewski, A.; Stanescu, D.; Ravelosona, D.; Jacqueline, A.S.; Chappert, C.; Rodmacq, B.; Diény, B. Magnetic logic using nanowires with perpendicular anisotropy. *Nanotechnology* **2009**, *20*, 215401. [CrossRef] [PubMed]
2. Parkin, S.S.P.; Yang, S.H. Memory on the racetrack. *Nat. Nanotechnol.* **2015**, *10*, 195–198. [CrossRef]
3. Awano, H. Investigation of domain wall motion in RE-TM magnetic wire towards a current driven memory and logic. *J. Magn. Magn. Mater.* **2015**, *383*, 50–55. [CrossRef]
4. Kim, K.J.; Yoshimura, Y.; Ono, T. Current-driven magnetic domain wall motion and its real-time detection. *Jpn. J. Appl. Phys.* **2017**, *56*, 0802A4. [CrossRef]
5. Bang, D.; Thach, P.V.; Awano, H. Current-induced domain wall motion in antiferromagnetically coupled structures: Fundamentals and applications. *J. Sci. Adv. Mater. Dev.* **2018**, *3*, 389–398. [CrossRef]
6. Parkin, S.S.P.; Hayashi, M.; Thomas, L.; Memory, M.D.-W.R. Magnetic Domain-Wall Racetrack Memory. *Science* **2008**, *320*, 190–194. [CrossRef] [PubMed]
7. Kläui, M.; Vaz, C.A.; Bland, J.A.C.; Wernsdorfer, W.; Faini, G.; Cambril, E.; Heyderman, L.J.; Nolting, F.; Rüdiger, U. Controlled and Reproducible Domain Wall Displacement by Current Pulses Injected into Ferromagnetic Ring Structures. *Phys. Rev. Lett.* **2005**, *94*, 106601. [CrossRef] [PubMed]
8. Hayashi, M.; Thomas, L.; Rettner, C.; Moriya, R.; Bazaliy, Y.B.; Parkin, S.S. Current Driven Domain Wall Velocities Exceeding the Spin Angular Momentum Transfer Rate in Permalloy Nanowires. *Phy. Rev. Lett.* **2007**, *98*, 037204. [CrossRef] [PubMed]
9. Hayashi, M.; Thomas, L.; Moriya, R.; Rettner, C.; Parkin, S.S. Current-Controlled Magnetic Domain-Wall Nanowire Shift Register. *Science* **2008**, *320*, 209–211. [CrossRef]
10. Tanigawa, H.; Koyama, T.; Yamada, G.; Chiba, D.; Kasai, S.; Fukami, S.; Suzuki, T.; Ohshima, N.; Ishiwata, N.; Nakatani, Y.; et al. Domain wall motion induced by electric current in a perpendicularly magnetized Co/Ni nano-wire. *Appl. Phys. Exp.* **2009**, *2*, 053002. [CrossRef]
11. Fukami, S.; Nakatani, Y.; Suzuki, T.; Nagahara, K.; Ohshima, N.; Ishiwata, N. Relation between critical current of domain wall motion and wire dimension in perpendicularly magnetized Co/Ni nanowires. *Appl. Phys. Lett.* **2009**, *95*, 232504. [CrossRef]
12. Boulle, O.; Kimmling, J.; Warnicke, P.; Kl, M.; R'udiger, U.; Malinowski, G.; Swagten, H.J.M.; Koopmans, B.; Ulysse, C.; Faini, G. Nonadiabatic spin transfer torque in high anisotropy magnetic nanowires with narrow domain walls. *Phys. Rev. Lett.* **2008**, *101*, 216601. [CrossRef]
13. Cormier, M.; Mougin, A.; Ferr'e, J.; Thiaville, A.; Charpentier, N.; Pi'echon, F.; Weil, R.; Baltz, V.; Rodmacq, B. Effect of electrical current pulses on domain walls in Pt/Co/Pt nanotracks with out-of-plane anisotropy: Spin transfer torque versus Joule heating. *Phys. Rev. B* **2010**, *81*, 024407. [CrossRef]
14. Moore, T.A.; Miron, I.M.; Gaudin, G.; Serret, G.; Auffret, S.; Rodmacq, B.; Schuhl, A.; Pizzini, S.; Vogel, J.; Bonfim, M. High domain wall velocities induced by current in ultrathin Pt/Co/AlOx wires with perpendicular magnetic anisotropy. *Appl. Phys. Lett.* **2008**, *93*, 262504. [CrossRef]
15. Emori, S.; Bauer, U.; Ahn, S.M.; Martinez, E.; Beach, G.S.D. Current-driven dynamics of chiral ferromagnetic domain walls. *Nat. Mater.* **2013**, *12*, 611–616. [CrossRef]
16. Ryu, K.S.; Thomas, L.; Yang, S.H.; Parkin, S.S.P. Chiral spin torque at magnetic domain walls. *Nat. Nanotechnol.* **2013**, *8*, 527–533. [CrossRef]
17. Ryu, K.-S.; Yang, S.-H.; Thomas, L.; Parkin, S.S.P. Chiral spin torque arising from proximity-induced magnetization. *Nat. Commun.* **2014**, *5*, 3910. [CrossRef]
18. Do, B.; Awano, H. Reversal of Domain Wall Motion in Perpendicular Magnetized Tb-Fe-Co Nanowires. *IEEE Trans. Magn.* **2013**, *49*, 4390–4393. [CrossRef]
19. Bang, D.; Yu, J.; Qiu, X.; Wang, Y.; Awano, H.; Manchon, A.; Yang, H. enhancement of spin Hall effect induced torques for current-driven magnetic domain wall motion: Inner interface effect. *Phys. Rev. B* **2016**, *93*, 174424. [CrossRef]
20. Kim, K.J.; Kim, S.K.; Hirata, Y.; Oh, S.H.; Tono, T.; Kim, D.H.; Okuno, T.; Ham, W.S.; Kim, S.; Go, G.; et al. Fast domain wall motion in the vicinity of the angular momentum compensation temperature of ferrimagnets. *Nat. Mater.* **2017**, *16*, 1187. [CrossRef]
21. Siddiqui, S.A.; Han, J.; Finley, J.T.; Ross, C.A.; Liu, L. Current-Induced Domain Wall Motion in a Compensated Ferrimagnet. *Phys. Rev. Lett.* **2018**, *121*, 057701. [CrossRef]
22. Caretta, L.; Mann, M.; Büttner, F.; Ueda, K.; Pfau, B.; Günther, C.M.; Hessing, P.; Churikova, A.; Klose, C.; Schneider, M.; et al. Fast current-driven domain walls and small skyrmions in a compensated ferrimagnet. *Nat. Nanotechnol.* **2018**, *13*, 1154–1160. [CrossRef]
23. Ranjbar, S.; Kambe, S.; Sumi, S.; Thach, P.V.; Nakatani, Y.; Tanabe, K.; Awano, H. Elucidation of the mechanism for maintaining ultrafast domain wall mobility over a wide temperature range. *Mater. Adv.* **2022**, *3*, 7028–7036. [CrossRef]

24. Li, P.; Kools, T.J.; Koopmans, B.; Lavrijsen, R. Ultrafast Racetrack Based on Compensated Co/Gd-Based Synthetic Ferrimagnet with All-Optical Switching. *Adv. Electron. Mater.* **2023**, *9*, 2200613. [CrossRef]
25. Tono, T.; Taniguchi, T.; Kim, K.J.; Moriyama, T.; Tsukamoto, A.; Ono, T. Chiral magnetic domain wall in ferrimagnetic GdFeCo wires. *Appl. Phys. Express* **2015**, *8*, 073001. [CrossRef]
26. Okuno, T.; Kim, D.H.; Oh, S.H.; Kim, S.K.; Nishimura, T.; Ham, W.S.; Futakawa, Y.; Yoshikawa, H.; Tsukamoto, A.; Tserkovnyak, Y.; et al. Spin-transfer torques for domain wall motion in antiferromagnetically coupled ferrimagnets. *Nat. Electron.* **2019**, *2*, 389–393. [CrossRef]
27. Berger, L. Exchange interaction between ferromagnetic domain wall and electric current in very thin metallic films. *J. Appl. Phys.* **1984**, *55*, 1954–1956. [CrossRef]
28. Li, Z.; Zhang, S. Domain-wall dynamics driven by adiabatic spin-transfer torques. *Phys. Rev. B* **2004**, *70*, 024417. [CrossRef]
29. Koyama, T.; Chiba, D.; Ueda, K.; Kondou, K.; Tanigawa, H.; Fukami, T.; Suzuki, N.; Ohshima, N.; Ishiwata, Y.; Nakatani, K.; et al. Observation of the intrinsic pinning of a magnetic domain wall in a ferromagnetic nanowire. *Nat. Mater.* **2011**, *10*, 194. [CrossRef]
30. Ishibashi, M.; Yakushiji, K.; Kawaguchi, M.; Tsukamoto, A.; Nakatsuji, S.; Hayashi, M. Reversal of current-induced domain wall motion in TbFeCo ferrimagnetic thin films across the magnetization compensation point. *Jpn. J. Appl. Phys.* **2023**, *62*, 013001. [CrossRef]
31. Caretta, L.; Avci, C.O. Domain walls speed up in insulating ferrimagnetic garnets. *APL Mater.* **2024**, *12*, 011106. [CrossRef]
32. Torrejon, J.; Kim, J.; Sinha, J.; Mitani, S.; Hayashi, M.; Yamanouchi, M.; Ohno, H. Interface control of the magnetic chirality in CoFeB/MgO heterostructures with heavy-metal underlayers. *Nat. Commun.* **2014**, *5*, 4655. [CrossRef] [PubMed]
33. Ranjbar, S.; Sumi, S.; Tanabe, K.; Awano, H. Evaluation of multi-bit domain wall motion by low current density to obtain ultrafast data rate in a compensated ferrimagnetic wire. *APL Mater.* **2022**, *10*, 091102. [CrossRef]